2022 44th Annual International Conference of
the IEEE Engineering in Medicine & Biology Society (EMBC)
Scottish Event Campus, Glasgow, UK, July 11-15, 2022

2022 44th Annual International Conference of the IEEE Engineering in Medicine & Biology Society (EMBC) | 978-1-7281-2782-8/22/$31.00 ©2022 IEEE | DOI: 10.1109/EMBC48229.2022.9871504

Cross-modal activation of the primary visual cortex by auditory stimulation in RCS rats: considerations in visual prosthesis

Daniel Caravaca-Rodriguez, Gregg J. Suaning, *Senior Member, IEEE*
Alejandro Barriga-Rivera, *Member, IEEE*

Abstract— An important brain re-wiring, the so-called cross-modal plasticity, occurs during progression of retinal degenerative diseases to compensate for lack of visual input. The visual cortex does not go 'unused', instead it is devoted to processing other sensory modalities. In this study we recorded, in the visual cortex, visual- and auditory-evoked potentials in an anesthetized murine model of retinal degeneration. The latency to the first peak of the recorded local field potentials was used to assess the speed of the response. Visual responses occurred significantly faster in the control group. Conversely, auditory responses appeared significantly faster in animals with retinal degeneration. This suggests the compensatory neural rewiring is optimizing the performance of other sensory modalities, hearing in this case. This phenomenon may play an important role in visual neuro-rehabilitation. Whether or not it can promote or deter the interpretation of artificially encoded neural signals from a visual prosthesis remains to be studied.

I. Introduction

The lack of neural activity that occurs as a consequence of loss or damage of a sensory input, typically hearing or sight, induces an important neuronal reorganization in the brain [1]. In blindness, auditory [2] and somatosensory [3] modalities acquire importance as a result of adaptation to the lack of visual sensations. The neurons in the occipital cortex, conceived to process visual information, become activated after auditory or tactile stimuli are presented. This neuroplastic phenomenon, known as cross-modal plasticity, allows the visually impaired to redeploy the processing power of the 'unused' brain areas to the processing of other sensory information [4]. Whether or not these neuroplastic changes benefit or deter the rehabilitation process that follows the reintroduction of a visual input, for example from a retinal implant, remains to be studied [5, 6].

The aim of this work was to provide an initial evaluation of the cross-modal activation of the visual cortex, in this case by auditory stimulation, in a murine model of retinal degeneration. The electrophysiological characterization of cross-modal activation will help understanding the neuronal rewiring that occurs in the brain and how it affects visual rehabilitation.

*Research supported by grant number RTI2018-094465-J-I00 funded by MICIN/AEI/10.13039/501100011033 and by "ERDF A way of making Europe". This work has also received the support of FUNDALUCE (Foundation for Fighting Blindness) and the Research and Transfer Plan of the Universidad de Sevilla. D. Caravaca-Rodriguez and A. Barriga-Rivera are with the Department of Applied Physics III, Universidad de Sevilla, 41092 Sevilla, Spain. G. J. Suaning is with the School of Biomedical Engineering, The University of Sydney, Sydney, Australia 2006. A. Barriga-Rivera is also with the School of Biomedical Engineering, The University of Sydney, Sydney, Australia 2006.
E-mail for correspondence: abrivera@us.es.

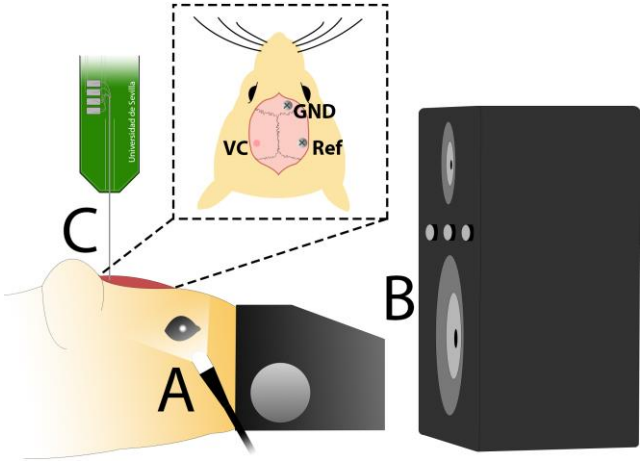

Figure 1. Schematic representation of the experimental setup. A, Visual stimuli were generated using a white LED. B, Auditory stimuli were generated using a broadband loudspeaker. C, with the animal anaesthetized, neural responses were recorded using a tetrode implanted in the visual cortex (VC). Ground (GND) and reference (Ref) screws electrodes were also implanted for differential amplification.

II. Methodology

All experimental procedures described herein were approved by the Ethics Committee of the Universidad de Sevilla, Spain, and were conducted following the European Directive 2010/63/EU on the protection of animals used for scientific purposes, and its corresponding transposition into the Spanish law (BOE-A-2013-1337).

Seven Royal College of Surgeon (RCS) rats were included in this study. Four animals (RCS *rdy-/-*), three males and one female, presented a recessive homozygous mutation that causes a progressive retinal degeneration (DYS-1: P42, DYS-2: P62, DYS-3: P63, DYS-4: P341). Three animals (RCS *rdy+/+*), two males and one female, had wild-type phenotype (CTR-1: P84, CTR-2: P301, CTR-3: P306,) and were used as control in this study. Note that an aged dystrophic animal, DYS-4, was included to verify the absence of visual response in the dystrophic strain.

A. Animal preparation and surgery.

Animals were sedated to reduce handling discomfort by placing them within a dark anesthetic chamber with increasing concentrations of isoflurane in oxygen (1 to 5 %). A mixture of ketamine (80 $mg \cdot kg^{-1}$) and xylazine (10 $mg \cdot kg^{-1}$) was then administered intraperitoneally to induce a surgical level of anesthesia. Anesthesia was later maintained *via* face mask, by delivering a constant flow of isoflurane in oxygen (1 - 2%) at approximately 400 $ml \cdot min^{-1}$. Two intramuscular injections of dexamethasone ($0.06\ mg \cdot kg^{-1}$) and

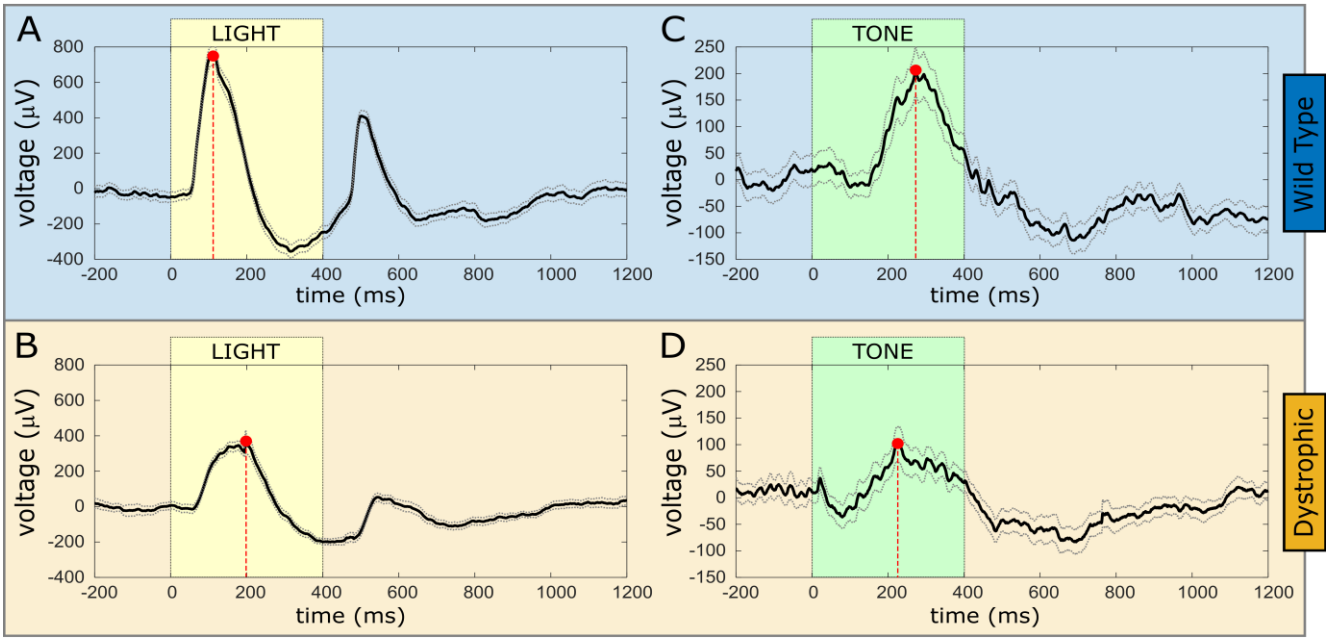

Figure 2. Examples of the ensemble average obtained from 50 repeats of the visually and auditory evoked potentials recorded from visual cortex in dystrophic and non-dystrophic RCS rats. A and B are visually evoked potentials recoded in sighted and dystrophic animals respectively following a 400-ms light pulse. C and D are the auditory evoked potentials in sighted and dystrophic animals respectively following a 400-ms tone at 32 kHz. Red dots indicate the peak value used to measure the latency of the response. Gray dotted lines represent the standard error of the mean.

amoxicillin/clavulanic acid (20/5 $mg \cdot kg^{-1}$) were also administered before surgery to reduce inflammatory responses and risk of infections respectively. Heart rate and oxygen saturation were continuously monitored using a UT100V pulse oximeter (Utech Co., Ltd, Magill, Australia). Body temperature was maintained at a nominal 37.5 ºC using a closed-loop custom temperature controller. Corneal hydration was maintained by periodically applying Carbomer 974P lubricant (Ursapharm, Saarbrücken, Germany) directly on the surface of the cornea. Lidocaine was sprayed inside ears before securing the head of the animal within a stereotaxic apparatus.

A midline incision was made on the skin to expose the surface of the skull. The periosteum was then retracted and the bone scraped to reveal the cranial sutures. Two burr holes were drilled to implant cranial screws which were used as ground (1.0 mm lateral to midline, 3.0 mm rostral to bregma) and reference (4.0 mm lateral to midline, 6.5 mm caudal to bregma) electrodes respectively, as illustrated in Fig. 1. A 2x1 mm^2 craniotomy was opened above the visual cortex (VC) following coordinates from Paxinos and Watson [7] (3.5 mm lateral to midline and 6.5 mm caudal to bregma, contralateral to the stimulated eye). The dura mater was then dissected away using a 21G needle with the tip bent in a 45-degree angle. An additional burr hole was opened above the optic chiasm (0.4 mm caudal to bregma and 0.2 mm lateral to midline) in DYS-4. A tetrode made from 50-µm Teflon-coated tungsten wires (Advent, Oxford, England) was then advanced to deliver electrical stimuli to the visual system.

B. Electrophysiological recordings.

Based on a previous work [8], local field potentials (LFPs) were recorded from the VC using custom tetrodes fabricated by twisting four 25-µm diameter insulated nichromium wires (Advent, Oxford, England) as described by Liao and coworkers [9]. The tips of the electrodes were then gold plated to reduce their impedance to below 500 kΩ. The electrodes were mounted on a custom PCB and interfaced to a RHS 32-channel headstage (Intan Technologies, Intan Technologies, California, USA). Neural signals were acquired at 30 kHz using a neural RHS stimulation/recording controller (Intan Technologies, California, USA).

C. Visual, auditory and electrical stimulation.

Visual stimuli were generated using a LX5093UWC/C white light emitting diode (LED) (Lumex, Illinois, USA) positioned approximately 10 mm from the cornea. The LED was powered using a DG1022z waveform source (Rigol, Gilching, Germany) to generate 5-V square waveforms, 400 ms in duration. A 200 Ω resistor was mounted in series to limit the current. Ambient illuminance was maintained below 1500 lux.

Auditory stimuli consisted of 400-ms tones of approximately 100 dBA, with frequencies between 500 Hz and 32 kHz. In doing so, a 1-V_{p-p} sinusoidal waveform was generated using a DG1022z waveform source and fed into an Adam A3X 2-way active studio monitor (ADAM Audio, Berlin, Germany) with frequency response between 60 and 50 kHz. Ambient noise was kept below 45 dBA. Each stimulus was repeated 50 times every 4013 ms to allow sufficient time for neural recovery to a baseline state, and to avoid synchronization with other devices. Additionally, in DYS-4, electrical stimuli were constant-current biphasic pulses with phase time set to 500 µs, 100 µA of amplitude, and no inter-phase delay. The stimuli were delivered using two paired channels of the RHS headstage. Inter-stimulus time was set to 1013 ms, and each stimulus was repeated 50 times.

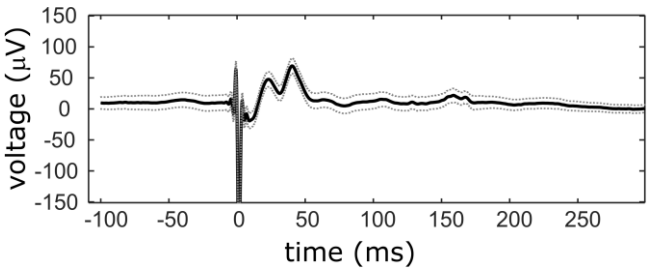

Figure 3. Ensemble average obtained from 50 repeats of the electrically evoked potentials recorded from the visual cortex of a rat with retinal degeneration (RCS rdy-/-, P:341). Electrical stimuli, delivered at t = 0, consisted of constant-current biphasic pulses, 100 μA in amplitude with 500 μs phase time. Gray dotted lines represent the standard error of the mean.

D. Data analysis

Data were analyzed in Matlab 2021a (Mathworks, Natick, Massachusetts) using custom scripts. Neural recordings were low-pass filtered to remove frequency components above 300 Hz using a fifth-order Butterworth filter with zero-phase. The assemble average of 50 repeats was then computed to estimate the overall response. The response latency, defined here as the time between the onset of the stimulus and the first peak of the response was measured. Errors were expressed as the standard error of the mean (SEM). Overall values were compared using the t-test, and given the small sample size of the cohorts, differences were considered statistically significant at the 90% level. Linear correlation was studied using the Pearson coefficient.

III. Results

Visually evoked potentials (VEPs) were successfully elicited in all non-dystrophic animals, including the aged one. The overall latency to the first peak was 98 ± 12 ms. VEPs were also successfully obtained in three dystrophic animals with overall latency to peak 201 ± 48 ms, as illustrated in the example shown in Fig. 2. Visual responses appeared significantly faster in non-dystrophic rats than in rats with retinal degeneration (*p-value* = 0.03). Note that due to the severe degree of retinal degeneration in DYS-4, VEPs could not be obtained from this animal. Instead, electrically evoked responses were successfully demonstrated to ensure recordings were obtained from the VC, as shown in Fig.3.

Similarly, auditory evoked potentials (AEPs) were elicited in all animals. Note these responses were also recorded in the VC. The overall response time, calculated by averaging the latencies obtained from all tones presented here, were 306 ± 40 ms and 266 ± 43 ms for wild type and dystrophic rats respectively. In this case, auditory responses appeared faster in animals with retinal degeneration than in those with the wild type phenotype (*p-value* = 0.001). Furthermore, the VEP latencies remained faster in the control group (*p-value* = 0.00) and in the animals with retinal degeneration (*p-value* = 0.08), exhibiting overall differences in the response latencies of 208 ms and 65 ms respectively. The frequency response analysis performed revealed that the strongest differences appeared at 32 kHz (*p-value* = 0.04), as shown in Fig. 4. Statistically significant differences were also demonstrated at 1 kHz (*p-value* = 0.10), 2 kHz (*p-value* = 0.08) and 8 kHz (*p-value* = 0.10). Differences at other frequencies did not reach significant levels. We also observed that the latencies decreased significantly with increasing frequencies from 4 kHz onwards, showing a strong linear correlation in the wild type phenotype (r^2=0.85), and a very strong correlation in the dystrophic strain (r^2=0.96) in a logarithmic frequency scale.

IV. Discussion and Conclusions

The absence of a sensory input is known to produce significant changes in the neural circuitries in charge of processing that information stream [10]. Other sensory modalities exploit the vacant neural resources by stablishing new cortico-cortical connections. In this study we have demonstrated electrophysiological differences between wild type animals and those with retinal degeneration. These differences are evidence of a more effective cross-modal connectivity between the neurons in the auditory system and the VC in the dystrophic rat. Note the electrodes used here were sufficiently small to record the LFPs elicited from the activation of the neurons in the VC only [11]. Furthermore, the latency differences between visually and auditory evoked responses, both recorded from the VC, suggest a subsequent activation of VC neurons by cross-modal projections from the neurons in the auditory system, typically in the auditory cortex, the thalamus, or both. To determine the contribution of each synaptic input, further anatomical studies, for example using retrograde neural tracers [12], are required to quantify the number and the quality of these new connections.

VEPs were used as a control test to assess the quality of visual perception of each research subject, and to compare visually and auditory evoked responses. Our results demonstrated delayed visual responses in dystrophic animals in agreement with those reported in the scientific literature [13, 14]. Note an important retinal remodeling occurs during retinal degeneration that alters the normal activation patterns of the neural cascade of the visual pathway. In turn, AEPs appeared faster in the dystrophic animals. This suggests a neural reorganization of the auditory neural pathways to promote an optimization of the hearing performance. Thus, faster auditory responses in dystrophic animals could be explained by a stronger contribution of newly stablished

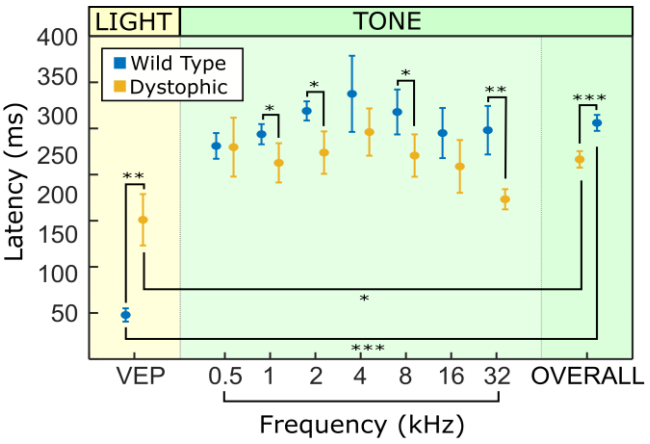

Figure 4. Mean latency from the stimulus onset to the first peak of the visually evoked potentials (VEP) and auditory evoked potentials. Responses were obtained to the presentation of 400-ms light pulses and tones of frequencies between 0.5 kHz and 32 kHz. *p-value < 0.1, **p-value < 0.05, and ***p-value < 0.01 from t-test.

thalamocortical connections [15]. It is worth noting that latencies tend to decrease with increasing sound pitches, reaching the quickest auditory response at 32 kHz. This correlation may be associated with a progressive approach to the frequency components of the vocalization range of the rat (20-70 kHz) [16]. It is also important to note that DYS-4 showed the quickest auditory responses in all frequencies of the range under examination. Perhaps, the extreme degree of retinal degeneration of this experimental subject explains said optimal responses. However, given that only one aged dystrophic animal was included in this study, solid conclusions cannot be drawn in this regards.

The sample size here was sufficient to demonstrate differences between dystrophic and control animals. However, further experimental subjects should be included in future studies to demonstrate differences at all frequency tones presented, and to determine potential sex-related differences. Note also this research was conducted under gaseous anesthesia. The use of isoflurane is known to reduce cortical responsiveness by decreasing the amplitude and the latency of the evoked potentials [17, 18]. In the study described herein, levels of anesthesia were maintained approximately constant throughout the entire experiment to reduce its potential impact in the neural recordings. Therefore, the results described here are expected to show more clear differences in further behaving animal studies.

Sound frequencies below 0.5 kHz were also tested, but were discarded as they caused important artifacts in the LFPs. It is possible to anticipate similar differences in the amplitude of the LFPs among the experimental groups in both, VEPs and AEPs: in dystrophic animals, VEPs are expected to be significantly weaker as a consequence of a reduction in the visual input, whereas AEPs are expected to be stronger as the result of newly formed connections. Unfortunately, comparisons could not be established due to differences in the amount of metal exposed at the tip of the electrodes and the subsequent different electrodes impedances obtained. Thus, the recording and the analysis of neural spikes, should smaller electrodes and intravenous anesthesia are used [19], may help overcoming some of these limitations in future studies.

As many prey animals, rodents rely mainly in the sense of smell, touch and hearing. Despite the limited vision these animals have, the lack of visual input can potentiate other senses [20], as reported in humans [21]. Therefore, the RCS rat seems to be a good model to study the role of these plastic changes in visual rehabilitation. Whether the establishment of new neuronal circuitries that exploit key visual processing centers, *i.e.* the VC, during the absence of visual inputs hampers the reintroduction of visual sensations needs to be studied. If techniques to manipulate said brain re-writing are developed, perhaps, these neuroplastic mechanisms can be modulated to improve the quality of the visual percepts elicited from a visual prosthesis, particularly facilitating better interpretations of artificially encoded neural messages [22].

REFERENCES

[1] J. U. Henschke *et al.*, "Early sensory experience influences the development of multisensory thalamocortical and intracortical connections of primary sensory cortices," *Brain Struct Funct,* vol. 223, no. 3, pp. 1165-1190, 2018.

[2] X. Meng, J. P. Y. Kao, H. K. Lee, and P. O. Kanold, "Intracortical circuits in thalamorecipient layers of auditory cortex refine after visual deprivation," *eNeuro,* vol. 4, no. 2, 2017.

[3] K. Abe and H. Yawo, "Quantitative study of the somatosensory sensitization underlying cross-modal plasticity," *PLoS One,* vol. 13, no. 12, p. e0208089, 2018.

[4] H.-K. Lee and J. L. Whitt, "Cross-modal synaptic plasticity in adult primary sensory cortices," *Curr Opin Neurobiol,* vol. 35, pp. 119-126, 2015.

[5] B. Heimler, N. Weisz, and O. Collignon, "Revisiting the adaptive and maladaptive effects of crossmodal plasticity," *Neuroscience,* vol. 283, pp. 44-63, 2014.

[6] M. Beyeler, A. Rokem, G. M. Boynton, and I. Fine, "Learning to see again: biological constraints on cortical plasticity and the implications for sight restoration technologies," *J Neural Eng,* vol. 14, no. 5, p. 051003, 2017.

[7] G. Paxinos and C. Watson, *The rat brain in stereotaxic coordinates: hard cover edition*. Elsevier, 2006.

[8] A. Barriga-Rivera *et al.*, "A 4+ 1 architecture for in vivo electrophysiology visual prosthesis," *J Access Des All,* pp. 81-101, 2016.

[9] Y.-F. Liao, M.-L. Tsai, C.-T. Yen, and C.-H. Cheng, "A simple method for fabricating microwire tetrode with sufficient rigidity and integrity without a heat-fusing process," *J Neurosci Methods,* vol. 195, no. 2, pp. 211-215, 2011.

[10] J. U. Henschke *et al.*, "Early sensory experience influences the development of multisensory thalamocortical and intracortical connections of primary sensory cortices," *Brain Struct Funct,* vol. 223, no. 3, pp. 1165-1190, 2018.

[11] Y. Kajikawa and C. E. Schroeder, "How local is the local field potential?," *Neuron,* vol. 72, no. 5, pp. 847-858, 2011.

[12] M.-H. Kim, P. Znamenskiy, M. F. Iacaruso, and T. D. Mrsic-Flogel, "Segregated subnetworks of intracortical projection neurons in primary visual cortex," *Neuron,* vol. 100, no. 6, pp. 1313-1321. e6, 2018.

[13] G. Lennerstrand, "Delayed visual evoked cortical potentials in retinal disease," *Acta Ophthalmol,* vol. 60, no. 4, pp. 497-504, 1982.

[14] J. F. Maya-Vetencourt *et al.*, "Subretinally injected semiconducting polymer nanoparticles rescue vision in a rat model of retinal dystrophy," *Nat Nanotechnol,* vol. 15, no. 8, pp. 698-708, 2020.

[15] G. Bronchti, P. Heil, R. Sadka, A. Hess, H. Scheich, and Z. Wollberg, "Auditory activation of 'visual'cortical areas in the blind mole rat (Spalax ehrenbergi)," *Eur J Neurosci,* vol. 16, no. 2, pp. 311-329, 2002.

[16] S. M. Brudzynski and N. H. Fletcher, *Rat ultrasonic vocalization: short-range communication* (Handbook of Behavioral Neuroscience). Elsevier, 2010, pp. 69-76.

[17] G. Sitdikova *et al.*, "Isoflurane suppresses early cortical activity," *Ann Clin Transl Neurol,* vol. 1, no. 1, pp. 15-26, 2014.

[18] J. Kortelainen *et al.*, "Effect of isoflurane on somatosensory evoked potentials in a rat model," in *Conf Proc IEEE Eng Med Biol Soc*, 2014: IEEE, pp. 4286-4289.

[19] A. Barriga-Rivera, V. Tatarinoff, N. H. Lovell, J. W. Morley, and G. J. Suaning, "Long-term anesthetic protocol in rats: feasibility in electrophysiology studies in visual prosthesis," *Vet Ophthalmol,* vol. 21, no. 3, pp. 290-297, 2018.

[20] Y. Zhou, F.-H. Fang, P. Pan, Z.-R. Liu, and Y.-H. Ji, "Visual deprivation induce cross-modal enhancement of olfactory perception," *Biochem Biophys Res Commun,* vol. 486, no. 3, pp. 833-838, 2017.

[21] F. Gougoux, F. Lepore, M. Lassonde, P. Voss, R. J. Zatorre, and P. Belin, "Pitch discrimination in the early blind," *Nature,* vol. 430, no. 6997, pp. 309-309, 2004.

[22] A. Barriga-Rivera, L. Bareket, J. Goding, U. A. Aregueta-Robles, and G. J. Suaning, "Visual prosthesis: interfacing stimulating electrodes with retinal neurons to restore vision," *Front Neurosci,* vol. 11, p. 620, 2017.